ON THE GOVERNING EQUATION FOR WEB TENSION WITH OUT-OF-ROUND ROLLS

By

Carlo Branca, Prabhakar R. Pagilla, and Karl N. Reid
Oklahoma State University
USA

ABSTRACT

In roll-to-roll (R2R) manufacturing the presence of non-ideal elements, such as out-of-round or eccentric rolls, induces periodical oscillations in the web tension signal. Model simulations based on ideal elements do not exhibit these tension oscillations but can only follow the measured tension signal in an average sense. In order for the models to predict these measured tension oscillations due to non-ideal elements, the derivation of governing equations must consider a mechanism to include the correct behavior of the non-ideal transport elements. Continuing with our previous work on this topic presented at previous IWEBs, we present additional results that provide improvements to the web span tension governing equation which can better predict measured tension signals. In particular, this work is useful for tension control in the unwind section of the web line when the unwind material roll is often out-of-round.

that are not associated with an imbalance in material flow. Second, the material flow rate is not proportional to the peripheral velocity of the web on the out-of-round roll and must be computed explicitly. Given a measure of out-of-roundness of the roll, due to the complexity of the problem it is difficult to derive a closed form expression for the material flow rate as a function of the roll position and velocity. A numerical algorithm for the computation of the material flow rate is presented in the paper. Based on the computation of the material flow rate and the algorithm for the computation of the span length adjacent to an out-of-round roll which was presented in the previous IWEB, a new governing equation for web tension is developed. Using this new governing equation a dynamic model for an experimental web line is developed and model simulations are conducted. To corroborate the model, experiments are conducted on the web line with an out-of-round unwind material roll. Comparison of the results from model simulations and experiments are presented and discussed.

NOMENCLATURE

A	Area of cross section of the web [ft^2]
C_G	Geometric center of the roller
C_R	Center of rotation of the eccentric roller
d_{ex}	Distance between the center of rotation and the web exit point on the roller [ft]
$d_{C_GC_R}$	Distance between the center of gravity and the center of rotation of the roller [ft]
E	Modulus of elasticity (Young's modulus) $\left[\frac{\text{lbf}}{\text{ft}^2}\right]$
g	Gravitational acceleration
L	Free span web length [ft]
ℓ	Length of material leaving the material roll [ft]
J	Roller inertia [lb ft^2]
m	Roller mass [lb]
R	Radius of the roller [ft]
T_i	Web tension in the i-th span [lbf]
v	Web velocity (or peripheral velocity of the roller) [FPM]
V	Material roll volume [ft^3]
w	Web width [ft]
ω	Roller angular velocity [rad/sec]
θ	Roller angular displacement [rad]
τ_u	Roller friction torque [lbf ft]
ρ	Web density [lb/ ft^3]

INTRODUCTION

The presence of non-ideal elements introduces periodical oscillations in web tension and web velocity that are not reproduced by computer simulations based on the models of the ideal elements, examples of modeling of web transport with ideal elements can be found in [1–3]. In our previous work [4] we showed that using the frequency content of

the measured tension signal, sources of tension and velocity oscillations can be identified and that the periodical oscillations may be paired with specific non-ideal rolls in the line. One key aspect highlighted in [4] is the fact that in the presence of a non-ideal roller the length of the web span adjacent to the non-ideal roller is time varying. In the derivation of the governing equation for web tension in a span adjacent to an ideal roller, it is assumed that the web span length is constant. In the case of a non-ideal roller this assumption is not true, and incorporation of this aspect leads to the following modified governing equation [4]:

$$\dot{T}_i = \frac{v_i(EA - T_i) - v_{i-1}(EA - T_{i-1}) + \dot{L}_i(EA - T_i)}{L_i} \qquad \{1\}$$

In order to numerically solve the differential equation an expression for the span length and span length derivative are needed. Algorithms for the computation of the span length in the presence of eccentric and out-of-round rollers are presented in [5]. The complete analysis, modeling and validation of the governing equation for web transport in the presence of eccentric rollers is presented in [6]. This paper covers the analysis, modeling and validation of web transport in the presence of an out-of-round material roll.

A summary of the algorithm for the computation of the span length for a convex shaped material roll will be presented first since the results from the algorithm will be used in several places throughout the paper. Then the necessary modification to the governing equation of web velocity will be presented. This includes three main adjustments to the governing equation derived using ideal behavior. First, the center of mass of the roll may not coincide with the center of rotation. In this case an additional torque due to gravity has to be included in the model. Second, the arm length of the torque due to the tension in the first span is not equal to the radius of the roll; it is time varying and must be computed for solving the velocity equations. Lastly, the expression for the roll inertia needs to be obtained and it differs from the case of the ideal roll. After including the modifications to the governing equations of web tension and web velocity, results from a series of experiments are shown to verify the proposed model. A discussion of the results obtained from the comparison of the experimental data with data from model simulations is given; since this comparison shows poor correlation between the two data, it is evident that the model needed further improvements and this is the motivation for the modification of the governing equation of web tension described in the second part of the paper. To understand the reasoning for this last modification one has to revert back to the first principles derivation of governing equations. In particular, the governing equation for web tension is obtained applying the law of conservation of mass for the control volume containing the web span, i.e., at any instant in time the variation of mass in the control volume is equal to the difference of entering and exiting material flow rate. In the case of an ideal roll it can be shown that the peripheral velocity of the web on the neighboring rolls is proportional to the material flow rate. A discussion about how in the presence of a non-ideal roll the peripheral velocity and the material flow rate are not proportional is given. An explicit expression for the material flow rate has to be computed instead, without relying on it being proportional to the peripheral velocity. The paper is concluded with a discussion of the comparison of the data from model simulations and experiments after an explicit expression for material flow rate is included in the model.

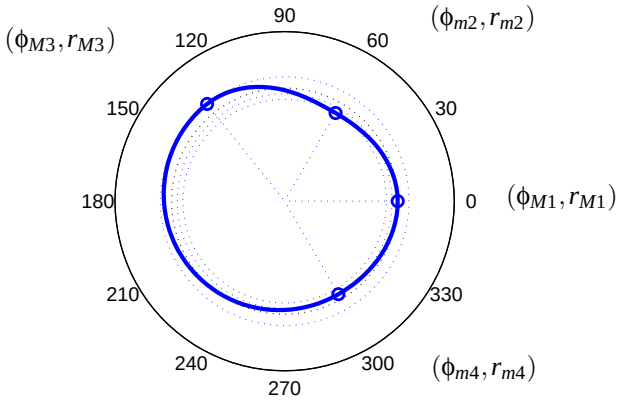

Figure 1: Characterization of a generic shaped material roll.

COMPUTATION OF SPAN LENGTH FOR CONVEX SHAPED MATERIAL ROLL

The problem of computing the length of a web span between a convex shaped material roll and a perfect idle roller is considered in this section. This problem may be divided into three sub-problems. First, given a convex shaped roll it is necessary to find a method to characterize the roller, which is to find a way to associate a parametric equation that is, at the same time, accurate enough to describe the surface of the roller but simple enough to allow the computations necessary for the subsequent steps. Second, once the equation describing the shape of the roller is obtained, it is necessary to obtain an equation for the tangent of the roller as a function of the angular displacement. Finally, an optimization problem must be formulated to find the equation for the line tangent to the convex shaped roller and the idle roller.

To describe the shape of the roller it is assumed that a list of all the maximum and minimum radii of the roll and their angular position with respect to a fixed coordinate axis is known; an illustration of this characterization is shown in Fig. 1. Note that the positions of the radius maximum and minimum are functions of the angular displacement of the roll θ. The algorithm for the computation of the span length is derived assuming that the roll is fixed. The modifications to the algorithm to account for the movement of the roll are discussed later in the section.

One possible approach to characterize the convex shape is to find a single function that can describe the entire profile of the roll; this approach leads to undue complexity. In fact, finding such a function is non-trivial and, moreover, the resulting function will be either a highly nonlinear function or a function with many parameters; this would also result in numerical implementation of subsequent steps to be more computationally intensive. To avoid this problem the characterization of the shape is done in intervals, that means a different function is used to describe the shape of the roller

between each minimum and maximum. In other words, given the list of the locations $(\phi_{m1}, \phi_{M1}, \phi_{m2}, \phi_{M2}, \ldots, \phi_{mn}, \phi_{Mn})$ and the values of minima and maxima of the radius $(r_{m1}, r_{M1}, r_{m2}, r_{M2}, \ldots, r_{mn}, r_{Mn},)$, the function takes the form:

$$r(\phi) = \begin{cases} r_1(\phi_{m1}, \phi_{M1}, r_{m1}, r_{M1}, \phi) & \text{if } \phi_{m1} \leq \phi \leq \phi_{M1}; \\ r_1(\phi_{M1}, \phi_{m2}, r_{M1}, r_{m2}, \phi) & \text{if } \phi_{M1} \leq \phi \leq \phi_{m2}; \\ \vdots & \\ r_{2n}(\phi_{Mn}, \phi_{m1}, r_{Mn}, r_{m1}, \phi) & \text{if } \phi_{Mn} \leq \phi \leq \phi_{m1}. \end{cases} \quad \{2\}$$

To guarantee that each junction point is an extreme point and in order to avoid any kind of discontinuity, each function r_i must be such that

$$\begin{aligned} r_i(\phi_{mj}) &= r_{i+1}(\phi_{mj}) = r(\phi_{mj}), \\ r_i'(\phi_{mj}) &= r_{i+1}'(\phi_{mj}) = 0. \end{aligned} \quad \{3\}$$

The resulting interpolation function is:

$$r(\phi) = (r(\phi_M) - r(\phi_m)) \left[-2\frac{(\phi - \phi_m)^3}{\Delta\phi^3} + 3\frac{(\phi - \phi_m)^2}{\Delta\phi^2} \right] + r(\phi_m). \quad \{4\}$$

Note that the same function may be used for intervals starting in a maximum and ending in a minimum by simply switching ϕ_m with ϕ_M.

The next step is to find an expression for the line tangent to the perimeter of the roller for any given point on the perimeter identified in polar coordinates by the pair $(\phi, r(\phi))$. Given the function $r(\phi)$ in $\{4\}$ rearranged in the form:

$$r(\phi) = \delta\phi^3 + \gamma\phi^2 + \beta\phi + \alpha, \quad \{5\}$$

the expression for the slope of the line tangent to the pair $(\phi, r(\phi))$ can be shown to be

$$\begin{aligned} m &= \frac{n_3\phi^3 + n_2\phi^2 + n_1\phi + n_0}{d_3\phi^3 + d_2\phi^2 + d_1\phi + d_0}, \\ n_0 &= \alpha\sin\phi - \beta\cos\phi, \quad n_1 = \beta\sin\phi - 2\gamma\cos\phi, \\ n_2 &= \gamma\sin\phi - 3\delta\cos\phi, \quad n_3 = \delta\sin\phi, \\ d_0 &= \alpha\cos\phi - \beta\sin\phi, \quad d_1 = \beta\cos\phi + 2\gamma\sin\phi, \\ d_2 &= \gamma\cos\phi + 3\delta\sin\phi, \quad d_3 = \delta\cos\phi. \end{aligned} \quad \{6\}$$

This expression will be used in the next step to setup the optimization problem that will be used to find the equation for the common line tangent to the material roll and the idle roller.

Among all the tangents to the convex shaped roller, the one which is tangent to the idle roll is the one having the distance to the center of the idle roller equal to the radius. This aspect may be exploited to setup an optimization problem to find the common tangent. Given a generic point on the surface of the material roll described in polar coordinates by $(\phi, r(\phi))$, the line tangent to the surface at that point is given by

$$\begin{aligned} y &= r(\phi)\sin\phi + m(x - r(\phi)\cos\phi), \\ \mathbf{t}(\phi) : y &- m(\phi)x + m(\phi)r(\phi)\cos\phi - r(\phi)\sin\phi = 0 \end{aligned} \quad \{7\}$$

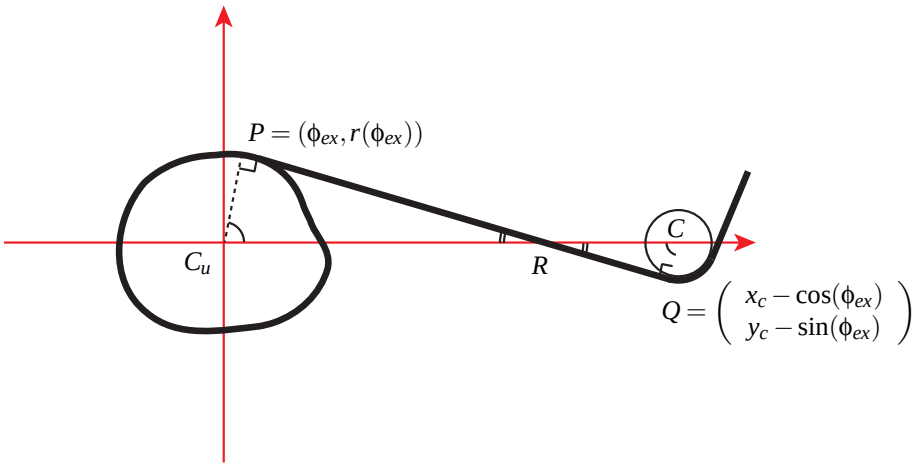

Figure 2: Computation of the web span extreme points. Because of the similarity of the triangles C_uRP and CRQ, the angles in C_u and C are equal.

with m as given in $\{6\}$.

The distance between the tangent $\mathbf{t}$ and the center of the roller C is

$$\mathbf{d}(\mathbf{t}(\phi), C) = \sqrt{\frac{|\alpha x_c + \beta y_c + \gamma|}{\alpha^2 + \beta^2}} \qquad \{8\}$$

where $\alpha = -m(\phi)$, $\beta = 1$ and $\gamma = m(\phi)r(\phi)\cos\phi - r(\phi)\sin\phi$.

By solving the optimization problem

$$\phi_{ex} = \min_{\phi} J(\phi) = \min_{\phi} (\mathbf{d}(\phi) - R)^2, \qquad \{9\}$$

a point $(\phi_{ex}, r(\phi_{ex}))$ is found on the generally shaped roller perimeter whose tangent distance from the center of the idle roller is equal to R. Notice that the optimization problem has two solutions, one corresponding to the over-wrap on the idle roller and the other to the under-wrap. A modified cost function $J_p(\phi)$ which has only one solution may be derived [5].

Once the optimization problem is solved, the coordinates of the exit point of the web on the roll $P = (\phi_{ex}, r(\phi_{ex}))$ are determined. The polar coordinates for P can easily be converted into Cartesian coordinates. Also, the coordinates of the contact point of the web on the downstream roller can be obtained as shown in Fig. 2. With the expressions for the extreme points P and Q of the web span, the computation of the length of the span is straight forward:

$$L = ||P - Q||. \qquad \{10\}$$

As explained earlier in the section, the algorithm has been derived without considering the movement of the roll. When the roll moves the positions of the minimum and

maximum radius on the roll change. Specifically, assuming that the original list of radius minima and maxima $\{(\phi_{m1}, r_{m1}), (\phi_{M1}, r_{M1}), \ldots, (\phi_{mn}, r_{mn},),$ $(\phi_{Mn}, r_{Mn})\}$ is given for the initial displacement of the roll $\theta(0) = 0$. Once the roll moves to a new position $\theta(t)$ the position of the radius minima and maxima will shift by an angle equal to $\theta(t)$. Therefore, the list of radius minima and maxima changes to $\{(\phi_{m1} + \theta(t), r_{m1},), (\phi_{M1} + \theta(t), r_{M1}), \ldots, (\phi_{mn} + \theta(t), r_{mn},), (\phi_{Mn} + \theta(t), r_{Mn})\}$ and the algorithm for the span length can be applied to the new list. Therefore, for any given angular displacement of the roll $\theta(t)$ the corresponding span length $L(\theta(t))$ can be computed.

Because it is not possible to obtain a closed form expression for the web span length, the inclusion of the effects of an out-of-round roll in the computer simulation is more complex compared to the case of the eccentric roller. The optimization problem can only be solved off-line before the computer simulation starts, but the optimization problem is completely defined only when the angular displacement is known. The angular displacement of the roll is obtained from the integration of the dynamic equation of the roll once the simulation starts. Moreover, the span length derivative $\dot{L}(t)$ that is required to solve the governing equation of tension cannot be obtained analytically, therefore, a numerical approximation for $\dot{L}(t)$ is required.

From these observations it is clear that in order to implement in model simulations the effects of the presence of the out-of-round roll, it is necessary to have a discretization of the angular displacement of the roll. By doing so, the optimization problem can be solved off-line before the simulation starts, and a look-up table can be used on-line to approximate the web span length when the simulation is running. Suppose the roll displacement is discretized with N equally distributed points, then the finite set of angular displacements is given by:

$$\Theta = \{\theta_1, \ldots, \theta_N\}, \qquad \theta_i = (i-1)\delta\theta, \qquad \delta\theta = \frac{2\pi}{N}. \tag{11}$$

The web span length for each angular position in Θ can be computed using the algorithm described in this section. The pairs $(\theta_i, L(\theta_i))$ will constitute a look-up table that can be used during the execution of the simulation to compute an approximation of the web span length and its derivative. In particular, suppose that at simulation time t_k the angular displacement $\theta(t_k)$ is obtained from the integration of the governing equations of velocity with $\theta_i \leq \theta(t_k) < \theta_{i+1}$, $\theta_i, \theta_{i+1} \in \Theta$, then the span length and span length derivative may be approximated with:

$$\begin{aligned} L(\theta(t_k)) &= L(\theta_i) + \frac{\theta_{i+1} - \theta(t_k)}{\theta_{i+1} - \theta_i}(L(\theta_{i+1}) - L(\theta_i)), \\ \dot{L}(\theta(t_k)) &= \frac{L(\theta(t_k)) - L(\theta(t_{k-1}))}{t_k - t_{k-1}}. \end{aligned} \tag{12}$$

In summary, because of the presence of the out-of-round material roll, the governing equation for web tension should include the effect of the time varying web span length. Therefore, equation $\{1\}$ must be used to simulate the effect of the presence of the non-ideal roll. The span length and its derivative cannot be computed in closed form, a numerical approximation is used instead and a procedure to obtain this numerical approximation was described in this section.

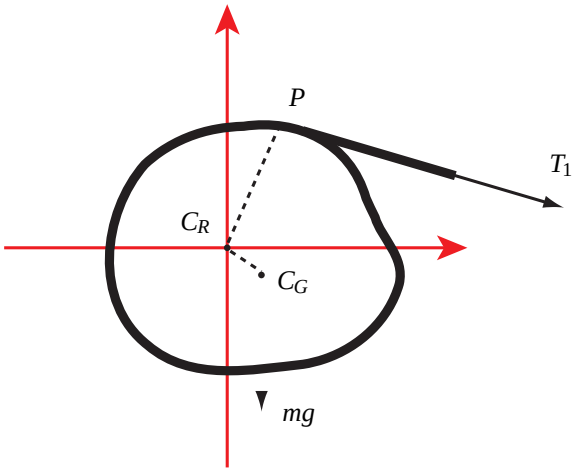

Figure 3: Sketch of the out-of-round roll and torques acting on it. Note: C_R is the center of rotation of the roll and C_G is its center of gravity.

MODIFIED GOVERNING EQUATION FOR WEB VELOCITY

In the presence of an out-of-round material roll the governing equation for web velocity needs to be modified as well. This is mainly due to three reasons: the location of the center of rotation may not coincide with the center of mass of the roll, the expression for the time varying inertia is different, and the torque due to web tension is not equal to $R_u T_1$. The necessary corrections to the governing equation for web speed to account for these aspects will be discussed in this section. A sketch of the out-of-round roll and all the torques acting on it is shown in Fig. 3. The new governing equations for the roll are

$$\begin{aligned} \dot{\theta} &= \omega, \\ J_u \dot{\omega} &= -\tau_f - d_{C_G C_R} mg \sin\theta - d_{ex} T_1 - \dot{J}_u \omega + \tau_u \end{aligned} \qquad \{13\}$$

where τ_f is the friction torque, $d_{C_G C_R}$ is the distance between the center of gravity and the center of rotation, m is the mass of the roll, g is the acceleration due to gravity, d_{ex} is the distance between the exit point of the web P and the center of rotation of the roll C_R, J_u is the total roll inertia and τ_u is the input torque. The remainder of the section explains how each term in $\{13\}$ is derived.

First, because of the out-of-roundness of the roll, it is possible that the center of mass of the roll is different from its center of rotation. In this case an extra torque term due to gravity needs to be added to the governing equation of the angular velocity. The equations to compute the center of gravity C_R of the roll are

$$\begin{aligned} \bar{x} &= \frac{\iint x \rho dA}{m} = \frac{\iint r^2(\phi)\cos(\phi)\rho(\theta) dr d\phi}{m}, \\ \bar{y} &= \frac{\iint y \rho dA}{m} = \frac{\iint r^2(\phi)\sin(\phi)\rho(\theta) dr d\phi}{m} \end{aligned} \qquad \{14\}$$

where $dA = r(\phi)d\phi dr$, ρ is the roll density, and $r(\phi)$ describe the roll in polar coordinates as described in the previous section. The lever arm of the torque due to gravity is given by the distance between the center of rotation C_R and the center of gravity $C_G = (\overline{x}, \overline{y})$.

The computation of the roll inertia is also more complex compared to the case of an ideal roll. The total moment of inertia is given by the sum of the core inertia, shaft inertia and the inertia due to the web. To obtain the component of the inertia due to the web J_w, it is necessary to start from the general expression for the computation of the moment of inertia:

$$J_w = \iiint_V \rho d^2(\phi)\mathbf{d}V = \rho \int_0^{w_w} \mathbf{d}\ell \iint_S d^2(\phi)\mathbf{d}S$$

where the infinitesimal volume $\mathbf{d}V = \mathbf{d}S\mathbf{d}\ell$. Since the function $d(\phi)$ does not vary along the width of the web, the integral along the width may be separated resulting in

$$J_w = \rho w_w \iint_S d^2(\phi)\mathbf{d}S = \rho w_w \int_0^{2\pi} \int_{R_c}^{r(\phi)} d^2(\phi)d(\phi)\,\mathbf{d}\phi\,\mathbf{d}d$$

where the infinitesimal area $\mathbf{d}S = d(\phi)\,\mathbf{d}\phi\,\mathbf{d}d(\phi)$ giving

$$\begin{aligned} J_w =& \rho w_w \int_0^{2\pi} \int_{R_c}^{r(\phi)} d^3(\phi)\,\mathbf{d}d\,\mathbf{d}\phi = \rho w_w \int_0^{2\pi} \frac{r^4(\phi) - R_c^4}{4}\,\mathbf{d}\phi \\ =& \rho w_w \left[\sum_{j=1}^{n-1} \int_{\phi_{m_j}}^{\phi_{M_j}} \frac{r_{2j-1}^4(\phi) - R_c^4}{4}\mathbf{d}\phi + \int_{\phi_{M_j}}^{\phi_{m_{j+1}}} \frac{r_{2j}^4(\phi) - R_c^4}{4}\mathbf{d}\phi \right] \\ &+ \rho w_w \left[\int_{\phi_{m_n}}^{\phi_{M_n}} \frac{r_{2n-1}^4(\phi) - R_c^4}{4}\mathbf{d}\phi + \int_{\phi_{M_n}}^{\phi_{m_1}} \frac{r_{2n}^4(\phi) - R_c^4}{4}\mathbf{d}\phi \right]. \end{aligned} \qquad \{15\}$$

The last expression for J_w in $\{15\}$ is obtained from the previous integral by using the definition of $r(\phi)$ given in $\{2\}$. Note that equation $\{15\}$ is obtained by considering J_w constant in time. The shape of the roll is defined using the location of the minimum and maximum radius $\{(\phi_{m1}, r_{m1}), (\phi_{M1}, r_{M1}), \ldots, (\phi_{mn}, r_{mn},), (\phi_{Mn}, r_{Mn})\}$, as the web is released the value of the radii decreases making J_w in $\{15\}$ time dependent. To obtain $J_w(t)$ it is necessary to obtain the interpolation functions $r_i(\phi)$ as in $\{4\}$ where now $r(\phi_m)$ and $r(\phi_M)$ are functions of time, and then explicitly solve the integral in $\{15\}$. However, since obtaining the time dependance of $r(\phi_m)$ and $r(\phi_M)$ is not practical, it is assumed that the web line is simulated for a short period of time such that the inertia can be considered constant and the term $\dot{J}_u$ in $\{13\}$ can be neglected.

The last modification to the governing equation of the angular velocity of the roll is to consider the changes in the arm length of the torque due to the tension, which is not equal to the radius of the roll but changes with time and depends on the point where the web leaves the roll. Clearly the arm length depends on the angular displacement of the roll and, similar to the web span length, derivation of a closed form expression is not feasible. The optimization problem described in the previous section to compute the span length can also be used to determine the arm length of the torque due to web tension. In fact, once the solution of the optimization problem ϕ_{ex} is obtained the arm length is simply given by $d_{ex}(\theta) = r(\phi_{ex}(\theta))$. From the implementation point of view, a look-up table may

be used for the arm length similar to the one for web span length. The same discretization of the angular displacement in $\{11\}$ is used to obtain the look up table for $d_{ex}(\theta)$.

The equations presented in this section are used to conduct model simulations in the presence of an out-of-round material roll. The next section describes the experiments that were performed to validate the model that includes only the time varying span length and the modified governing equation for web velocity.

EXPERIMENTS AND MODEL SIMULATIONS WITHOUT EXPLICIT COMPUTATION OF MATERIAL FLOW RATE

Roll imperfections are commonly seen in the web handling industry, these include, for example, a flat spot due to the roll being laid on the floor for an extended period of time, or an elliptically shaped roll as a consequence of holding a heavy roll on mandrels causing the bottom portion of the material to bulge due to gravity or improper winding in a process line. In order to verify the proposed model with a roll that clearly contains a flat spot, a material roll was made by winding material on top of a wooden insert as shown in Fig. 5. The wooden insert was designed so that the resulting out-of-round roll would mimic a roll with a flat spot. The profile of the wooden insert is shown in Fig. 4(a). The equations that describe the profile of the wooden insert in Cartesian coordinates are

$$\begin{cases} y = (r+t_f)\sqrt{1-\left(\frac{x-\ell_f/2}{r-\ell_f/2}\right)^2}, & -r \le x \le -\ell_f/2, \\ y = r+t_f & -\ell_f/2 \le x \le \ell_f/2, \\ y = (r+t_f)\sqrt{1-\left(\frac{x+\ell_f/2}{r-\ell_f/2}\right)^2}, & \ell_f/2 \le x \le r, \\ y = -\sqrt{r^2-x^2}, & -r \le x \le r \end{cases} \quad \{16\}$$

where r is the inner radius of the wooden insert, ℓ_f is the length of the flat spot, and t_f is the thickness of the wooden insert. The resulting out-of-round roll is shown in Fig. 4(b). In order to use the procedure described in the previous section for the computation of the span length and its derivative, it is required to obtain the list of maximum and minimum radii in order to divide the profile in segments. Normally one would measure the roll radius to identify the maxima and minima, in this case since the roll is made artificially out-of-round this information can be obtained analytically by transforming the Cartesian coordinates of the roll profile in equation $\{16\}$ into polar coordinates. A plot of the profile in polar coordinates is shown in Fig. 5(a), from the plot the list of the radius minima and maxima can be easily established. Figure 5(b) shows a comparison between the real profile of the flat spot and the interpolation obtained using the suggested procedure, the interpolation closely approximates the real profile.

Using the model proposed in this chapter a computer model simulation is set up to simulate a large web line running with the unwind roll shown in Fig. 4(b). The results from the experiment are shown in Fig. 6; it is evident there is little correlation between the two data. This clearly shows that some effects are neglected in the model simulation and provided a motivation for the need for additional analysis of the model in the presence of an out-of-round roll. One key issue that is responsible for this discrepancy in the data is discussed in the next section.

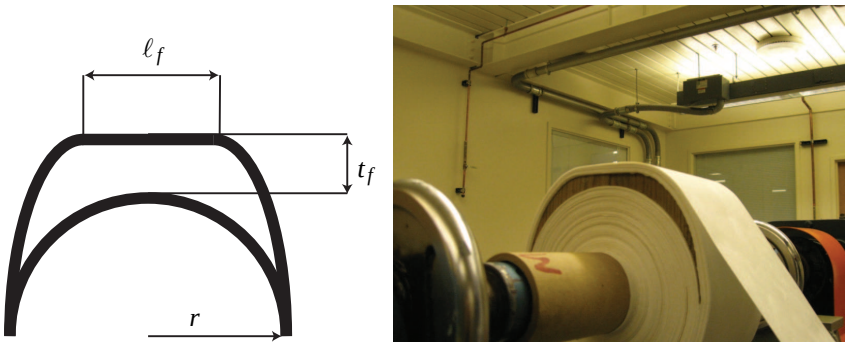

(a) Wooden insert profile. (b) Resulting out-of-round roll.

Figure 4: Design of the wooden insert to mimic a flat spot. The values chosen for the design are r =5.5in , ℓ_f =3in and t_f =0.5in

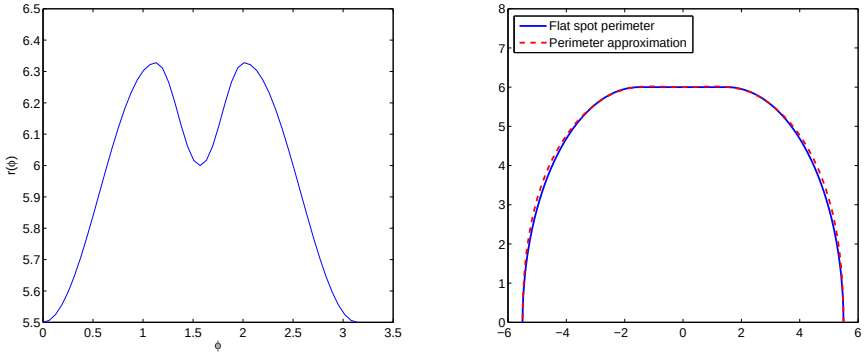

(a) Plot of the radius as function of the angular displacement for the flat spot profile. (b) Comparison of the flat spot profile with the interpolation obtained from the suggested procedure

Figure 5: Flat spot profile and its approximation.

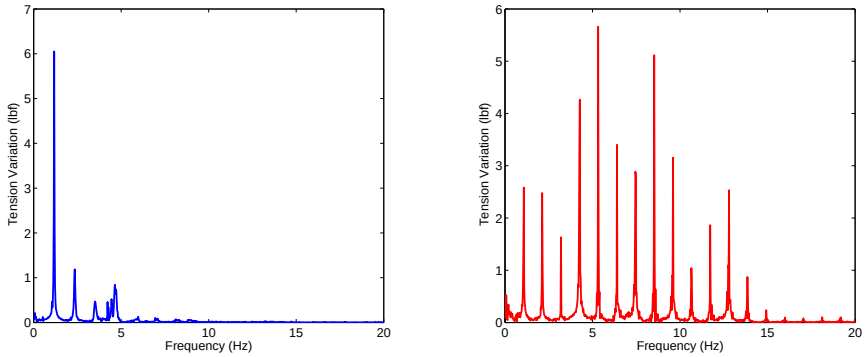

(a) FFT of the experimental data.

(b) FFT of the simulated model data.

Figure 6: Comparison between experimental and simulation data at 200 FPM with wooden insert simulating a flat spot.

COMPUTATION OF MATERIAL FLOW RATE IN THE PRESENCE OF AN OUT-OF-ROUND MATERIAL ROLL

The derivation of the web tension governing equation in $\{1\}$ is based on the conservation of mass in the control volume defined by the web span. In the governing equation for web tension $\{1\}$ it is assumed that v_{i-1} and v_i, the peripheral velocities of the web on the entry and exit rollers of the span, are proportional to the material flow rate entering and leaving the control volume. It can be shown that this assumption may not hold in the presence of a non-ideal roll.

Consider the extreme situation of a square roller as shown in Fig. 7. When the roller moves from the position in Fig. 7(a) to the position in Fig. 7(b) there is clearly no material transfer into the control volume of the web span, however, the peripheral velocity of the web on the roller is not zero. It is clear that in this situation the peripheral velocity of the web on the roller cannot be used to describe the material flow from the roller to the control volume of the web. The mass balance equation for the control volume can be expressed in its most general form is:

$$\frac{d}{dt}\int_{x_{i-1}(t)}^{x_i(t)} \rho(x,t)A(x,t)dx = \frac{dm_{in}}{dt} - \frac{dm_{out}}{dt} \qquad \{17\}$$

where now the material flow rate in the right hand side appears explicitly instead of the peripheral velocity. For an ideal roller, the relationship between the material flow rate and the peripheral velocity can be obtained in a straight forward manner as:

$$\frac{dm}{dt} = \frac{d}{dt}(\rho V(t)) = \rho\frac{dV}{dt} = \rho\frac{d}{dt}(A\ell(t)) = \rho A\frac{d\ell}{dt} = \rho A\frac{d}{dt}(R\theta(t)) = \rho AR\dot{\theta} = \rho Av(t) \qquad \{18\}$$

where $d\ell$ is the length of the infinitesimal segment of material dm that moved from the surface of the roller into the control volume in the infinitesimal time interval dt. The

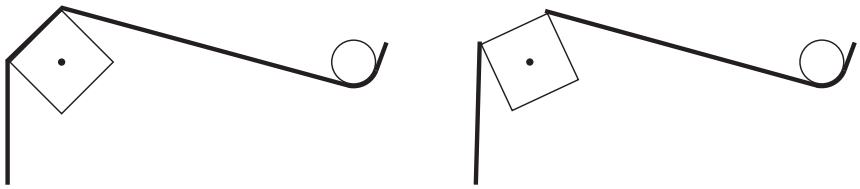

(a) Span with square roller at time t.

(b) Span with square roller at $t+dt$.

Figure 7: Example of a span with a square roller. In this situation the square roller rotates from the position at time t to the position at time $t+dt$ but there is no material flow into the span from the square roller.

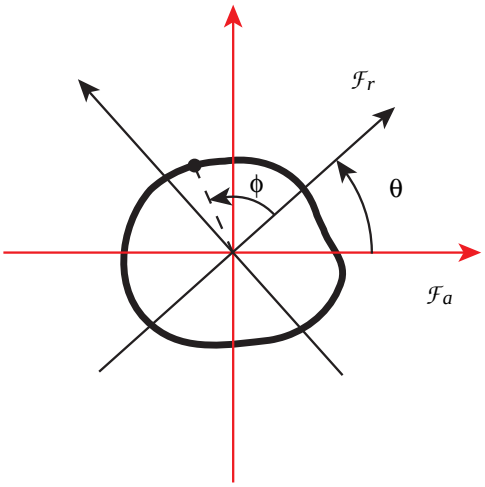

Figure 8: Definition of the absolute frame $\mathcal{F}_a$ and the relative frame $\mathcal{F}_r$.

reason for using the peripheral velocity for ideal rollers to describe the material flow rate is the relationship between $d\ell$ and the angular displacement $d\theta$. For a non-ideal roll the relationship between ℓ and θ is not as simple as in the case of the ideal roll.

Assuming the shape of a roller is given in polar coordinates $(r(\phi),\phi)$, then a procedure to find an expression for the material flow rate can be obtained. Two coordinate frames must be defined first. The first coordinate frame $\mathcal{F}_a$ is absolute and time invariant; this is the coordinate frame with respect to which the angular displacement of the roller is measured. The second coordinate frame $\mathcal{F}_r$ is a relative coordinate frame that moves together with the roller; this is the coordinate frame in which the polar coordinates of the roller are defined. An example of these two coordinate frames for a non-ideal roller is given in Fig. 8. The reason for requiring two coordinates frame will be clarified later. Note that the angular displacement of the roller is indicated by θ whereas ϕ is used to denote the angular position of a point on the perimeter of the roller in its polar coordinates in the frame $\mathcal{F}_r$.

Consider a non-ideal roller and a span adjacent to it as shown in Fig. 9. Let A be

the point at which the web makes contact with the roller at time t and the corresponding angle be $\phi_{en}(t)$ with respect to $\mathcal{F}_r$ as shown in Fig. 9(a). At time $t+dt$, let B be the web entry point on the roller and $\phi_{en}(t+dt)$ be the angle of B with respect to $\mathcal{F}_r$. When the roller rotates from the position in Fig. 9(a) at time t to the position in Fig. 9(b) at time $t+dt$, the infinitesimal segment of material dm that leaves the control volume of the web span is given by

$$dm = \rho dV = \rho A d\ell \qquad \{19\}$$

where $d\ell$ is the web length between the points B and A as shown. The length $d\ell$ can be computed by using the formula for the perimeter of a curve in polar coordinates. Given the curve $\mathcal{C} \equiv (r(\phi),\phi)$ in polar coordinates, the arc length ℓ_c between the two points $(r(\phi_1),\phi_1)$ and $(r(\phi_2),\phi_2)$ is given by

$$\ell_c = \int_{\phi_1}^{\phi_2} \sqrt{r^2(\phi) + \left(\frac{dr}{d\phi}\right)^2}\, d\phi. \qquad \{20\}$$

Note that to use the expression in $\{20\}$ the curve is required to be time invariant. This is the reason why the relative reference frame needs to be introduced, otherwise the curve would be varying with time in the absolute reference frame and it is not possible to compute $d\ell$. Using $\{20\}$ to compute the length $d\ell$ gives

$$d\ell = \int_{\phi_{en}(t)}^{\phi_{en}(t+dt)} \sqrt{r^2(\phi) + \left(\frac{dr}{d\phi}\right)^2}\, d\phi. \qquad \{21\}$$

Equation $\{21\}$ is the most general expression to compute length change which can be used to compute the rate of web material entering and exiting the web span.

One can verify whether the expression in $\{21\}$ for $d\ell$ is valid for the ideal roller case. An ideal roller in polar coordinates is described by $r(\phi) = R$. Moreover, since the point where the web makes contact with the roller does not change in the absolute reference frame, $\phi_{en}(t+dt)$ can be easily obtained as

$$\phi_{en}(t+dt) = \phi_{en}(t) + d\theta.$$

Substituting this expression in $\{21\}$ gives

$$d\ell = \int_{\phi_{en}(t)}^{\phi_{en}(t+dt)} \sqrt{r^2(\phi) + \left(\frac{dr}{d\phi}\right)^2}\, d\phi = \int_{\phi_{en}(t)}^{\phi_{en}(t)+d\theta} R d\phi = R d\theta$$

which leads to the same expression for $d\ell$ that was obtained in $\{18\}$.

From the discussion in the previous paragraph it is clear that in the governing equation of web tension $\{1\}$, the peripheral velocity of the web on the roll v_i must be replaced by $d\ell_i/dt$ with $d\ell$ as in $\{21\}$ whenever the roll i is a non-ideal roll. The correct form of equation $\{1\}$ is

$$\dot{T}_i = \frac{d\ell_i/dt(EA - T_i) - d\ell_{i-1}/dt(EA - T_{i-1}) + \dot{L}_i(EA - T_i)}{L_i}. \qquad \{22\}$$

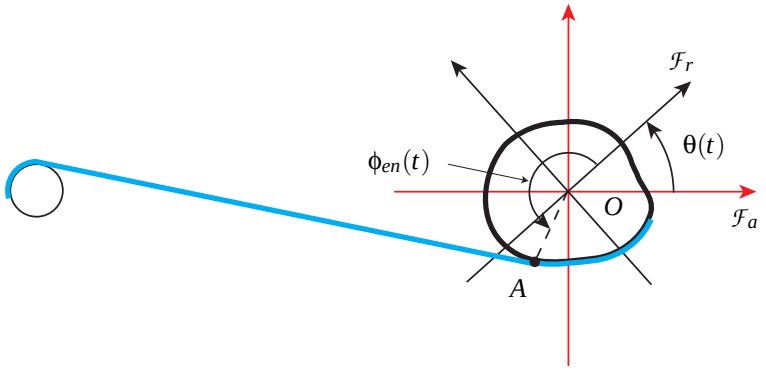

(a) Non-ideal roller at time t.

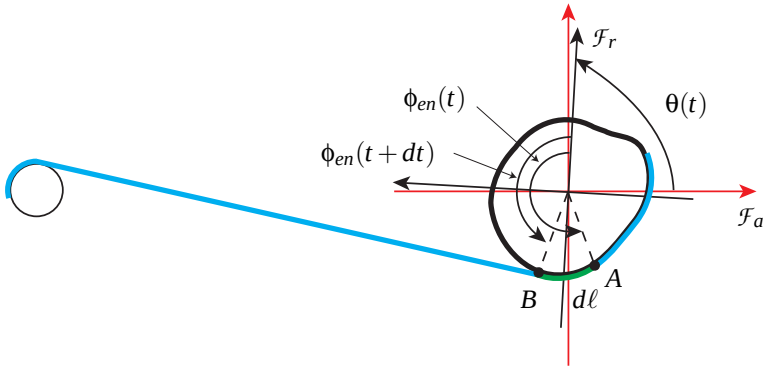

(b) Non-ideal roller at time $t+dt$.

Figure 9: Example of an out-of-round roller showing the length ($d\ell$) of web leaving the span in time dt.

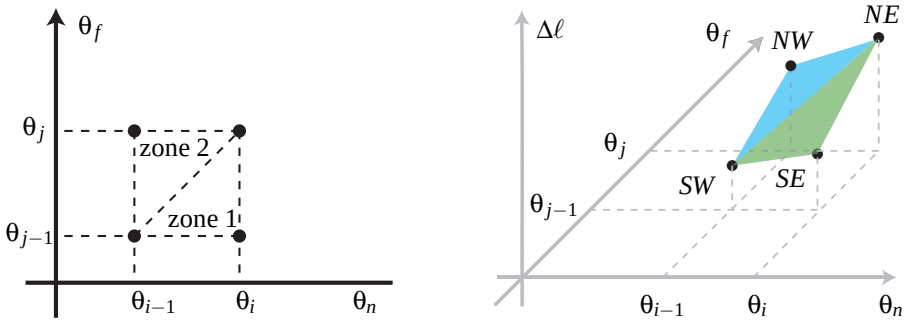

(a) Division of the area defined by the square $\{\theta_{i-1},\theta_i\}\times\{\theta_{j-1},\theta_j\}$ in the two zones.

(b) Construction of the two interpolation planes.

Figure 10: Construction of the interpolation function for $\Delta\ell$.

In order to solve equation $\{22\}$, the value of $d\ell/dt$ is required. Both $\phi_{en}(t)$ and $\phi_{en}(t+dt)$ in equation $\{21\}$ depend on the angular displacement $\theta(t)$ and they are computed numerically by solving the optimization problem introduced earlier in the paper. Hence, the integral in $\{21\}$ cannot be solved off-line. For this reason it is necessary to develop an approximation of equation $\{21\}$ that uses a discretization of the angular displacement θ in a similar manner to what was done for the computation of the span length L. In particular, the same discretization for θ in $\{11\}$ used for the computation of L is used for the computation of the approximation for $d\ell$. For every point θ_i in the set Θ the corresponding value of ϕ_i can be obtained from the solution of the optimization problem. For every pair $(\theta_i,\theta_j)\in\Theta$ with $j>i$, the length of the span $\Delta\ell$ entering the control volume when the roll moves from θ_i to θ_j can be computed by

$$\Delta\ell(\theta_i,\theta_j)=\int_{\phi_i}^{\phi_j}\sqrt{r^2(\phi)+\left(\frac{dr}{d\phi}\right)^2}\,d\phi. \qquad \{23\}$$

Note that for all pairs (θ_i,θ_j) with $j<i$, $\Delta\ell(\theta_i,\theta_j)=-\Delta\ell(\theta_j,\theta_i)$. The value obtained from equation $\{23\}$ can be arranged in a table where the element $\Delta\ell(i,j)=\Delta\ell(\theta_i,\theta_j)$. This table can be used during the simulation to compute an approximate value for $d\ell/dt$.

Assuming that at simulation time t_{k-1} the value of the angular displacement is θ_{k-1} with $\theta_i<\theta_{k-1}<\theta_{i+1}$ and that at time t_k the angular displacement is θ_k with $\theta_j<\theta_k<\theta_{j+1}$, since no value for the movement from θ_{k-1} to θ_k is defined in the table for $\Delta\ell$, it is necessary to define an interpolation function to define the value of $\Delta(\theta_{k-1},\theta_k)$ given the discretized values $\Delta\ell(i-1,j-1)$, $\Delta\ell(i-1,j)$, $\Delta\ell(i,j-1)$ and $\Delta\ell(i,j)$ in the $\Delta\ell$ table.

First, the space for the interpolation in $\mathbb{R}^3$ is defined by the coordinates $\mathbb{L}\equiv(\theta_n,\theta_f,\Delta\ell)$ where θ_n is the initial angular displacement, θ_f is the final angular displacement, and $\Delta\ell$ is the length of the span entering the control volume when the roll moves from θ_n to θ_f. Given the pair (θ_{k-1},θ_k), using the table for $\Delta\ell$ four points in $\mathbb{L}$ are defined: $SW\equiv(\theta_{i-1},\theta_{j-1},\Delta\ell(i-1,j-1))$, $NW\equiv(\theta_{i-1},\theta_j,\Delta\ell(i-1,j))$, $SE\equiv(\theta_i,\theta_{j-1},\Delta\ell(i,j-1))$ and $NE\equiv(\theta_i,\theta_j,\Delta\ell(i,j))$, see Fig. 10(b). For simplicity and to ensure continuity of the interpolation function, a linear interpolation is chosen.

However, given four independent points in a three dimensional space it is not possible to find a single plane that contains all the points. For this reason the square defined by $(\theta_{i-1},\theta_{j-1}),(\theta_{i-1},\theta_j),(\theta_i,\theta_{j-1}),(\theta_i,\theta_j)$ is split into two zones (see Fig. 10(a)). If the combination (θ_{k-1},θ_k) belongs to zone 1, then the interpolation is from the plane defined by the points $\{SW,SE,NE\}$, otherwise the interpolation is from the plane defined by the points $\{SW,NW,NE\}$, see Fig. 10(b). Once the three points $\{P_1,P_2,P_3\}$ that define the plane are determined, the vector orthogonal to the plane is given by

$$n \equiv \begin{pmatrix} n_x \\ n_y \\ n_z \end{pmatrix} = (P_2 - P_1) \times (P_3 - P_1). \qquad \{24\}$$

All the points on the plane defined by $\{P_1,P_2,P_3\}$ satisfy the equation

$$x(n_x - P_{1_x}) + y(n_y - P_{1_y}) + z(n_z - P_{1_z}) = 0. \qquad \{25\}$$

Therefore, the value of the interpolation function for (θ_{k-1},θ_k) is

$$\Delta\ell(\theta_{k-1},\theta_k) = -\frac{1}{n_z - P_{1_z}} \left[\theta_{k-1}(n_x - P_{1_x}) + \theta_k(n_y - P_{1_y})\right]. \qquad \{26\}$$

This procedure can be used to compute an on-line approximation of $d\ell/dt$ in $\{22\}$ during the execution of the model simulation.

A new computer model simulation was implemented for the EWL with the initial governing equation for tension $\{1\}$ replaced by the new governing equation $\{22\}$. The objective of this new simulation is to verify if the modified governing equation leads to a better correlation between the experimental and the model simulation data. The results of the new simulation are shown in Fig. 12. With the modified governing equation for web tension there is a better correlation between the two data.

Moreover, it can now be explained why the results from the simulation in Fig. 6(b) show larger oscillations compared to the experimental data. First Fig. 11(a) shows the difference between the peripheral velocity of the web and the material flow rate, the peripheral velocity has small variations while the material flow rate has large variations in proximity of the flat spot area. Figure 11(b) shows the span length variations which show similar variations in proximity of the flat spot. Note that the tension oscillations are a result of both the effects of span length variation and incoming/outgoing material flow rate. In the first simulation the governing equation for tension uses the peripheral velocity and the span length variations, while the second simulation uses the equivalent material flow rate and the span length variations. Figure 11(a) and Fig. 11(b) indicates how some of the span length variations are compensated by an increase in the equivalent material flow rate. When using the the peripheral velocity this compensation does not take place which explains the higher amplitude in the oscillations. This further demonstrates why one must use the equivalent material flow rate instead of the peripheral velocity in the governing equation of tension in order to appropriately simulate the system.

CONCLUSIONS AND FUTURE WORK

The derivation of the governing equations for web tension and roller angular velocity in the presence of an out-of-round material roll is described in this paper. Results from

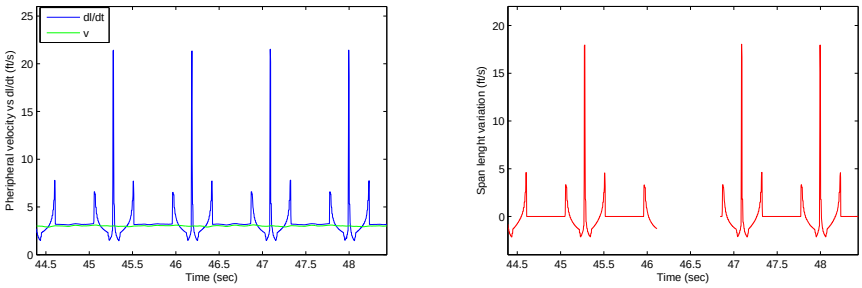

(a) Peripheral velocity vs $d\ell/dt$.

(b) Span length variations.

Figure 11: Example of how the use of the peripheral velocity neglects a significant amount of material flow in the case of a roll with a flat spot.

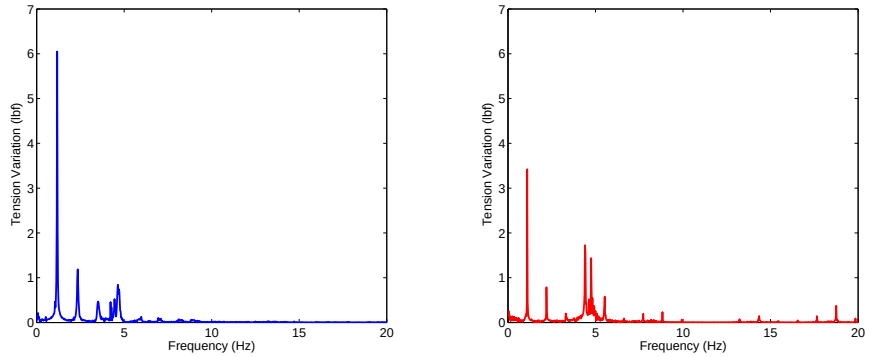

(a) FFT of the experimental data.

(b) FFT of the simulated data.

Figure 12: Comparison between experimental and simulation data at 200 FPM with wooden insert simulating a flat spot using modified governing equation for web tension.

previous work are used for validation of the governing equation for web transport in the presence of an out-of-round material roll. Apart from the inclusion of the span length variation in the governing equation of web tension, another aspect had to be considered. The derivation of the governing equation for web tension is based on the conservation of mass in the control volume encompassing the span. For an ideal roll the material flow rate in the control volume is proportional to the peripheral velocity of the web on the roll; this is not true for an out-of-round material roll. A closed form expression for the material flow rate could not be found, a numerical algorithm was presented.

The proposed model for the out-of-round roll was validated by comparing the data from model simulations with experimental data from the Euclid Web Line platform.

Analysis, modeling and validation of other primitive elements such as accumulators or other non-ideal elements will be the focus of the future work.

ACKNOWLEDGEMENTS

This work was supported by the Web Handling Research Center, Oklahoma State University, Stillwater, Oklahoma.

REFERENCES

1. Branderburg, G., "New mathematical model for web tension and register error," in Proceedings of the 3rd IFAC Conference Instrumentation Automation Paper, Rubber Plastic Industry, 1977, pp. 411–438.
2. Shelton, J. J., "Dynamic of web tension control with velocity or torque," in Proceedings of the American Control Conference, 1986, pp. 1423–1427.
3. Pagilla, P. R., Siraskar, N. B., and Dwivedula, R. V., "Decentralized control of web processing lines," IEEE Transactions on Control Systems Technology, vol. 15, January 2007, pp. 106–116.
4. Branca, C., Pagilla, P. R., and Reid, K. N., "Modeling and identification of the source of oscillations in web tension," Proceedings of the Tenth Intl. Web Handling Conference, 2009.
5. Branca, C., Pagilla, P. R., and Reid, K. N., "Computation of span length variations due to non-ideal rolls," Proceedings of the Tenth Intl. Web Handling Conference, 2009.
6. Branca, C., Pagilla, P. R., and Reid, K. N., "Governing Equations for Web Tension and Web Velocity in the Presence of Nonideal Rollers," Journal of Dynamic Systems, Measurement, Control, vol. 135(1), 2013.